CONFIDENTIAL

Copy 136
RM L54G01

C.2

NACA

RESEARCH MEMORANDUM

EXPERIMENTAL INVESTIGATION OF THE FORCES AND MOMENTS DUE TO SIDESLIP OF A SERIES OF TRIANGULAR VERTICAL- AND HORIZONTAL-TAIL COMBINATIONS AT MACH NUMBERS OF 1.62, 1.93, AND 2.41

By Donald E. Coletti

Langley Aeronautical Laboratory
Langley Field, Va.

NATIONAL ADVISORY COMMITTEE
FOR AERONAUTICS

WASHINGTON
August 5, 1954

CONFIDENTIAL

NATIONAL ADVISORY COMMITTEE FOR AERONAUTICS

RESEARCH MEMORANDUM

EXPERIMENTAL INVESTIGATION OF THE FORCES AND MOMENTS DUE TO SIDESLIP OF A SERIES OF TRIANGULAR VERTICAL- AND HORIZONTAL-TAIL COMBINATIONS AT MACH NUMBERS OF 1.62, 1.93, AND 2.41

By Donald E. Coletti

SUMMARY

An experimental investigation was made at Mach numbers of 1.62, 1.93, and 2.41 of a series of tail combinations consisting of a triangular vertical tail attached symmetrically to a triangular horizontal tail to determine the lateral force, yawing moment, and rolling moment due to sideslip. The apex angles of both the vertical- and horizontal-tail surfaces were varied systematically in order to obtain results for an appreciable range of operating conditions.

The results of the investigation indicated that, for tails having subsonic leading edges and supersonic trailing edges, the lateral-force derivative and the yawing-moment derivative were predicted satisfactorily by the method presented in NACA TN 3071 except when the leading edges approach a sonic condition. The theoretical rolling-moment derivative was in fair agreement with the experimental derivative. For the limited tests in which both the leading and trailing edges were supersonic, the prediction of the lateral-force derivative and the yawing-moment derivative obtained from NACA TN 2412 was in good agreement with the experimental derivatives, whereas the prediction of the rolling-moment derivative was fair.

INTRODUCTION

In reference 1, theoretical predictions are made of the lateral force, yawing moment, and rolling moment due to sideslip of a triangular vertical-tail surface attached symmetrically to a triangular horizontal-tail surface. These predictions are confined to configurations having subsonic leading edges and supersonic trailing edges. The theoretical

methods presented in reference 2 include a determination of the derivatives for the same geometric configurations as those in reference 1 but having supersonic leading and trailing edges. Within certain limitations, the theory may be extended to either rectangular or sweptback plan forms.

The purpose of the present investigation was to provide experimental results at supersonic speeds of the sideslip derivatives of a series of triangular vertical- and horizontal-tail combinations with a systematic variation of apex angles for each tail surface and, in turn, to assess the theoretical predictions presented in references 1 and 2 by comparison with the experimental results. The tests were made at Mach numbers of 1.62, 1.93, and 2.41 which, in combination with the range of apex angles, provided an appreciable range of operating conditions.

SYMBOLS

A_H aspect ratio of horizontal tail, $\frac{b_H^2}{S_H} = 4 \tan \gamma$

A_V aspect ratio of vertical tail, $\frac{b_V^2}{S_V} = 2 \tan \epsilon$

$B = \sqrt{M^2 - 1}$

β angle of sideslip, deg

b_H span of horizontal tail, in.

b_V span of vertical tail, in.

c_r common root chord of vertical and horizontal tail, in.

ϵ apex angle of vertical tail, deg

γ half apex angle of horizontal tail, deg

Y lateral force (see fig. 3)

N yawing moment (see fig. 3)

L' rolling moment (see fig. 3)

C_Y lateral-force coefficient, $\frac{Y}{\frac{1}{2}\rho V^2 S_V}$

C_n yawing-moment coefficient, $\frac{N}{\frac{1}{2}\rho V^2 b_V S_V}$

C_l rolling-moment coefficient, $\frac{L'}{\frac{1}{2}\rho V^2 b_V S_V}$

$C_{Y_\beta} = \left(\frac{\partial C_Y}{\partial \beta}\right)_{\beta \longrightarrow 0}$, per radian

$C_{n_\beta} = \left(\frac{\partial C_n}{\partial \beta}\right)_{\beta \longrightarrow 0}$, per radian

$C_{l_\beta} = \left(\frac{\partial C_l}{\partial \beta}\right)_{\beta \longrightarrow 0}$, per radian

V free-stream velocity, ft/sec

M free-stream Mach number

R Reynolds number per unit length, $\frac{\rho V}{\mu}$

S_H area of horizontal tail, sq in.

S_V area of vertical tail, sq in.

t thickness of tail surfaces, in.

ρ free-stream density, slugs/cu in.

μ coefficient of viscosity

Subscripts:

H horizontal tail

V vertical tail

[redacted]

APPARATUS

Wind Tunnel

The Langley 9-inch supersonic tunnel is a continuous-operation, closed-circuit type in which the pressure, temperature, and humidity of the enclosed air can be regulated. Different test Mach numbers are provided by interchangeable nozzle blocks which form test sections approximately 9 inches square. Eleven fine-mesh turbulence-damping screens are installed in the 5-feet-square settling chamber ahead of the supersonic nozzle.

Models

The steel test models consisted of a series of 18 triangular-tail combinations, where each combination included a triangular vertical tail mounted symmetrically on a triangular horizontal tail. A sketch of a typical model is shown in figure 1, and the various tail-shape parameters may be found in table I. The tails were fastened to a conical sting which, in turn, was mounted on a sting-type strain-gage balance. The apex angle of the vertical tails ϵ was varied between 20° and 35°. Each vertical tail was mounted on a horizontal tail of half apex angle γ varying from approximately 5° to 35°. A photograph of the series of 18 triangular-tail combinations is shown in figure 2.

A total bevel angle of 18° was machined on all the leading edges of the tails. The trailing edges of tails 1 to 17 remained blunt because it was felt that the blunt tailing edges would create little or no adverse effect on the measured sideslip derivatives. For tail 18, the bevel angle of 18° was machined on all edges. This particular tail was tested at an earlier date in a preliminary investigation and is included for the purpose of illustrating what may be expected for the condition of supersonic leading edges.

Balances

Two sting-type strain-gage balances were used in measuring the sideslip derivatives of the tails. One balance measured the lateral force (normal to the sting and balance longitudinal axis) and the yawing moment, whereas the other balance measured the rolling moment. Both balances were approximately 5 inches long and 5/8 inch in diameter. During the testing, each was mounted in an airtight housing with the front of the housing being fitted with a streamline windshield. The nose of the windshield was the same diameter as the base of the conical sting. (See fig. 1.) A gap of approximately 0.010 inch was maintained between the windshield and sting.

[redacted]

TESTS

Tests were conducted at Mach numbers of 1.62, 1.93, and 2.41. Measurements were made of the lateral force, yawing moment, and rolling moment for each triangular vertical- and horizontal-tail combination. A sketch of the tail showing the positive direction of velocities, forces, and moments is shown in figure 3. The average Reynolds numbers for all the tails tested at any particular Mach number are 360,000 per inch at $M = 1.62$, 320,000 per inch at $M = 1.93$, and 260,000 per inch at $M = 2.41$. One test was also made with tail 18 at $M = 1.62$ and at a Reynolds number of 690,000 per inch. The angle of sideslip of each configuration was measured optically by means of a light reflected from a small mirror mounted flush on the vertical-tail surface, as shown by figure 1. The range of angle of sideslip was approximately $\pm 5^\circ$. (The angle of attack was 0° for all tests.)

Throughout the tests, the dewpoint in the tunnel was maintained at a level where condensation effects would be negligible.

PRECISION OF DATA

The precision of the various quantities involved in the testing is listed in table II. The estimated uncertainties in a given quantity obtained from the strain-gage balances were combined by the method which follows from the theory of least squares outlined in reference 3. For the case where the precision varies with the angle of sideslip, the accuracy was determined at the approximate end of linearity. The uncertainties of the strain-gage data are presented as averages of all tails because the variation of the inaccuracies was random.

The accuracy of stream Mach number represents a maximum variation about a mean Mach number throughout the test section.

PRESENTATION OF RESULTS

The sideslip coefficients C_Y, C_n, and C_l of all the tail combinations are presented in figures 4 to 7 as a function of angle of sideslip measured in degrees. All the coefficients are based on the total area of the vertical tail.

The results shown in figure 4 are for those tails which were tested at $M = 1.62$ and a Reynolds number of 360,000 per inch, whereas figure 5 presents the results for $M = 1.93$ and $R = 320{,}000$ per inch.

[redacted]

The sideslip coefficients for tail 18 are shown in figures 6 and 7. The results shown in figure 6 are for a Mach number of 1.62 and Reynolds number of 360,000 per inch and 690,000 per inch. In figure 7, the results are for $M = 1.93$ with $R = 320{,}000$ per inch, and $M = 2.41$ with $R = 260{,}000$ per inch.

A summation of the experimental and theoretical lateral-force, yawing-moment, and rolling-moment curve slopes for each tail due to sideslip, expressed in radians, is given in table III along with the values of BA_V and BA_H.

DISCUSSION OF RESULTS

Tails 1 to 17, Subsonic Leading Edges

Lateral-force derivative C_{Y_β}.- A comparison between the theoretical and experimental values of BC_{Y_β} for various values of BA_H and BA_V is shown in figure 8. The values for the theoretical curves were computed by using the actual BA_V for each tail rather than the average value listed under the parts of figure 8. The theoretical value for $BA_H = 0$ was obtained by using the average BA_V. This value is shown in order to complete the trend established by the dashed theoretical curve for the decreasing aspect ratio of the horizontal tail. In figure 8 and in subsequent figures, a value of $BA_H = 4$ represents a condition where the leading edges of the horizontal tail are sonic; a value of $BA_V = 2$ represents the same condition for the vertical tail. As seen by figure 8, the agreement between experiment and the theory from reference 1 is very good with the exception of the place where the leading edge of the vertical tail approaches a sonic leading edge $(BA_V \approx 1.81)$. This agreement is understandable since linear theory predicts high pressure peaks for configurations with sonic leading edges.

Yawing-moment derivative C_{n_β}.- With the yawing moment taken about an axis through the apex of the tail combination (see fig. 3), a comparison between the theoretical and experimental values of C_{n_β} for various values of BA_H and BA_V is shown in figure 9. The computations for the theoretical values were made in the same manner as were those in connection with figure 8. The comparison between the theoretical and experimental C_{n_β} is very good with the exception of where the leading edge of

the vertical tail approaches a sonic condition $(BA_V \approx 1.81)$. The agreement for C_{n_β} at $BA \approx 1.81$, however, is better than for BC_{Y_β} at $BA_V \approx 1.81$.

Rolling-moment derivative C_{l_β}.- A comparison between the theoretical and experimental values of BC_{l_β} for various values of BA_H and BA_V is shown in figure 10. The agreement in trend is good but the agreement in magnitude, although fair, is not so good as that shown in the comparison between the theoretical and experimental results of BC_{Y_β} and C_{n_β}. Again, the same tendency toward poorer agreement as the leading edges approach a sonic condition is evident. The cause for the poorer overall agreement between experiment and theory for BC_{l_β} as compared with BC_{Y_β} and C_{n_β} is not known; however, it is possible that the presence of the conical sting may alter significantly the carry-over pressures on the horizontal-tail surfaces which are included in the theoretical rolling-moment prediction but are neglected, of course, in the lateral-force and yawing-moment calculations. It is also possible that the linearized theoretical evaluation of the induced loads created by the vertical tail and acting on the horizontal tail may not be indicative of the actual load as measured by experiment. In the calculations of the lateral force and yawing moment, no induced loads are involved and the comparison with the experiment in these cases shows the theoretical estimates to be satisfactory. For the rolling moment, however, both the induced rolling moments and the rolling-moment contribution of the vertical tail must be considered, and as shown by the experimental results, the agreement is only fair and could indicate that a linearized evaluation of the induced rolling moment may not be satisfactory.

Tail 18, Subsonic and Supersonic Leading Edges

Inasmuch as the geometric parameters for this tail do not fit into the systematic pattern of variation for tails 1 to 17, the results for this tail $(BC_{Y_\beta}, C_{n_\beta}$, and $BC_{l_\beta})$ are presented separately in figure 11. In addition, the range of test conditions for this tail gives both a subsonic and a supersonic leading edge. For the subsonic-leading-edge condition, the comparison between experiment and theory of the lateral force, yawing moment, and rolling moment is good at $M = 1.62$. At $M = 1.93$, however, the agreement is only fair and is due to the fact that the leading edges of both tail surfaces are approaching closely a sonic condition. At $M = 1.62$, tests of this tail were conducted at two different Reynolds numbers. As seen from figure 11, the absolute

values obtained at R = 690,000 per inch are only slightly different from those obtained at the lower Reynolds number.

For the case where the leading edges of the vertical and horizontal tails are supersonic (M = 2.41), the agreement between theoretical and experimental BC_{Y_β} and C_{n_β} is very good, whereas the prediction of BC_{l_β} is only fair. This discrepancy in the rolling moment is probably due to the same causes as those mentioned in connection with the tails having subsonic leading edges. In view of the fact that only one tail was tested having supersonic leading edges, it can only be stated that the theory of reference 2 was satisfactory for the particular test condition. There is, however, no apparent reason why equally satisfactory predictions could not be expected over a wide range of operating conditions.

CONCLUDING REMARKS

An investigation has been made at Mach numbers of 1.62, 1.93, and 2.41 of the sideslip derivatives of a series of triangular vertical- and horizontal-tail combinations with a systematic variation of apex angles for each tail surface. For tail combinations having subsonic leading edges and supersonic trailing edges, the prediction of the lateral-force derivative and yawing-moment derivative presented in NACA TN 3071 is in very good agreement with the experimental results except when the leading edges approach a sonic condition. The magnitude of the rolling-moment derivative is not predicted as well as the lateral-force and yawing-moment derivatives but the experimental trend of rolling-moment derivative with aspect ratio or Mach number is nevertheless in good agreement with the experimental variation.

The tests made of a tail combination having both supersonic leading and trailing edges were very limited and, as such, should not be taken as a sufficient assessment of the theory presented in NACA TN 2412 for the whole range of operating variables. For the tail combination investigated, however, the agreement between the experimental and theoretical lateral-force derivative and yawing-moment derivative is very good, whereas the prediction of the rolling-moment derivative is fair.

Langley Aeronautical Laboratory,
National Advisory Committee for Aeronautics,
Langley Field, Va., June 17, 1954.

REFERENCES

1. Malvestuto, Frank S., Jr.: Theoretical Supersonic Force and Moment Coefficients on a Sideslipping Vertical- and Horizontal-Tail Combination With Subsonic Leading Edges and Supersonic Trailing Edges. NACA TN 3071, 1954.

2. Martin, John C., and Malvestuto, Frank S., Jr.: Theoretical Force and Moments Due to Sideslip of a Number of Vertical Tail Configurations at Supersonic Speeds. NACA TN 2412, 1951.

3. Michels, Walter C.: Advanced Electrical Measurements. Second ed., D. Van Nostrand Co., Inc., 1941.

[redacted]

TABLE I.- TAIL-SHAPE PARAMETERS

[See fig. 1]

Tail	ϵ, deg	γ, deg	b_V, in.	b_H, in.	c_r, in.	t_V, in.	t_H, in.	A_V	A_H
1	19.97	5.04	1.563	0.759	4.300	0.060	0.030	0.7270	0.3530
2	20.29	9.89	1.588	1.497	4.295	.060	.060	.7394	.6971
3	20.46	14.88	1.605	2.286	4.302	.060	.060	.7462	1.0628
4	20.22	20.03	1.581	3.129	4.291	.060	.060	.7369	1.4584
5	20.27	25.13	1.568	3.984	4.246	.060	.060	.7386	1.8766
6	20.39	35.19	1.589	6.028	4.274	.060	.060	.7436	2.8207
7	25.42	4.98	1.840	.675	3.872	.060	.030	.9504	.3486
8	25.27	10.17	1.838	1.396	3.894	.060	.060	.9440	.7170
9	25.34	14.95	1.849	2.086	3.905	.060	.060	.9470	1.0683
10	24.79	20.46	1.802	2.912	3.902	.060	.060	.9236	1.4926
11	25.43	25.02	1.855	3.641	3.901	.060	.060	.9510	1.8667
12	35.25	4.94	2.266	.555	3.206	.060	.030	1.4136	.3462
13	35.48	10.05	2.272	1.130	3.187	.060	.060	1.4258	.7092
14	35.54	14.98	2.270	1.701	3.178	.060	.060	1.4286	1.0705
15	35.52	20.06	2.285	2.338	3.201	.060	.060	1.4277	1.4608
16	35.47	24.99	2.280	2.983	3.200	.060	.060	1.4250	1.8643
17	35.41	35.01	2.279	4.491	3.206	.060	.060	1.4217	2.8016
18	30.07	29.82	2.017	3.993	3.483	.060	.060	1.1582	2.2928

[redacted]

TABLE II.- SUMMARY OF TOTAL UNCERTAINTIES

Quantity	Accuracy for $C_Y = 0$	Accuracy at approximate end of linearity
C_Y	±0.0010	±0.0014
C_n	±.0015	±.0022
C_l	±.0003	±.0004
Initial angle of sideslip, deg	±.03	-------
Relative angle of sideslip, deg	±.01	-------
Mach number	±.01	-------
Reynolds number, per inch	±4,000	-------
Stream pressure, percent	±1.5	-------

[redacted]

TABLE III.- SUMMARY OF LATERAL-FORCE, YAWING-MOMENT, AND ROLLING-MOMENT CURVE SLOPES DUE TO SIDESLIP

M	Tail	BA_V	BA_H	Experiment			Theoretical		
				BC_{Y_β}, radian	C_{n_β}, radian	BC_{l_β}, radian	BC_{Y_β}, radian	C_{n_β}, radian	BC_{l_β}, radian
1.62	1	0.9266	0.4499	-1.884	2.762	-0.7450	-1.876	2.700	-0.7934
1.62	2	.9424	.8884	-2.096	2.979	-.7158	-2.159	3.054	-.7978
1.62	3	.9510	1.3545	-2.308	3.186	-.5770	-2.327	3.263	-.6967
1.62	4	.9392	1.8588	-2.359	3.335	-.4017	-2.397	3.403	-.5103
1.62	5	.9414	2.3918	-2.440	3.467	-.1753	-2.446	3.464	-.3026
1.62	6	.9477	3.5951	-2.578	3.742	.1315	-2.491	3.504	-.0032
1.62	12	1.8016	.4413	-2.827	2.131	-1.139	-2.987	2.211	-1.364
1.62	13	1.8172	.9038	-3.016	2.286	-1.132	-3.298	2.420	-1.403
1.62	14	1.8208	1.3644	-3.236	2.464	-1.125	-3.496	2.560	-1.381
1.62	15	1.8196	1.8618	-3.353	2.510	-1.081	-3.634	2.663	-1.311
1.62	16	1.8162	2.3761	-3.382	2.556	-.9641	-3.718	2.729	-1.210
1.62	17	1.8120	3.5707	-3.491	2.642	-.7888	-3.796	2.793	-1.005
1.93	1	1.2001	.5828	-2.422	2.687	-.9554	-2.353	2.614	-.9966
1.93	2	1.2206	1.1507	-2.667	2.894	-.9128	-2.678	2.925	-.9904
1.93	3	1.2317	1.7543	-2.805	3.031	-.7473	-2.862	3.098	-.8655
1.93	4	1.2164	2.4074	-2.913	3.232	-.5486	-2.928	3.209	-.6551
1.93	5	1.2192	3.0978	-2.980	3.300	-.3405	-2.973	3.252	-.4738
1.93	7	1.5688	.5755	-2.734	2.332	-1.0783	-2.814	2.392	-1.241
1.93	8	1.5584	1.1835	-3.027	2.682	-1.0783	-3.129	2.677	-1.228
1.93	9	1.5632	1.7635	-3.150	2.779	-.9932	-3.314	2.826	-1.147
1.93	10	1.5247	2.4638	-3.301	2.876	-.8513	-3.379	2.955	-.9535
1.93	11	1.5699	3.0815	-3.301	2.859	-.6810	-3.485	2.960	-.8593
1.62	18	1.4761	2.9223	-3.009	2.722	-.6574	-3.351	3.027	-.8046
1.62	[a]18	1.4761	2.9223	-3.068	2.848	-.6646	-3.351	3.027	-.8046
1.93	18	1.9118	3.7849	-3.311	2.309	-.7756	-3.908	2.725	-1.0697
2.41	18	2.5396	5.0276	-3.719	1.931	-.9046	-3.999	2.100	-1.1811

[a] R = 690,000 per inch.

[redacted]

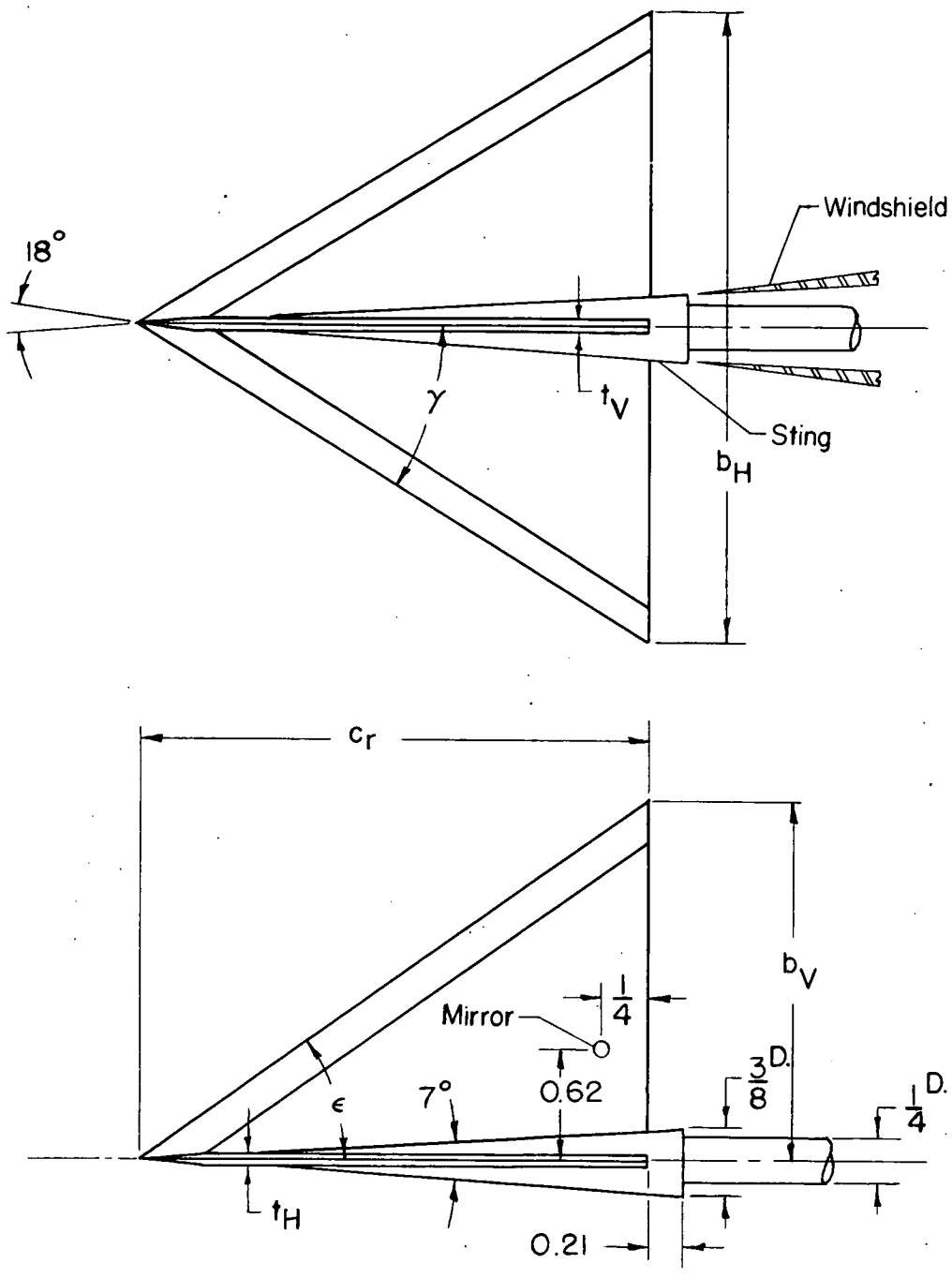

Figure 1.- Sketch of model. Tail-shape parameters are listed in table I. All dimensions are in inches.

[redacted]

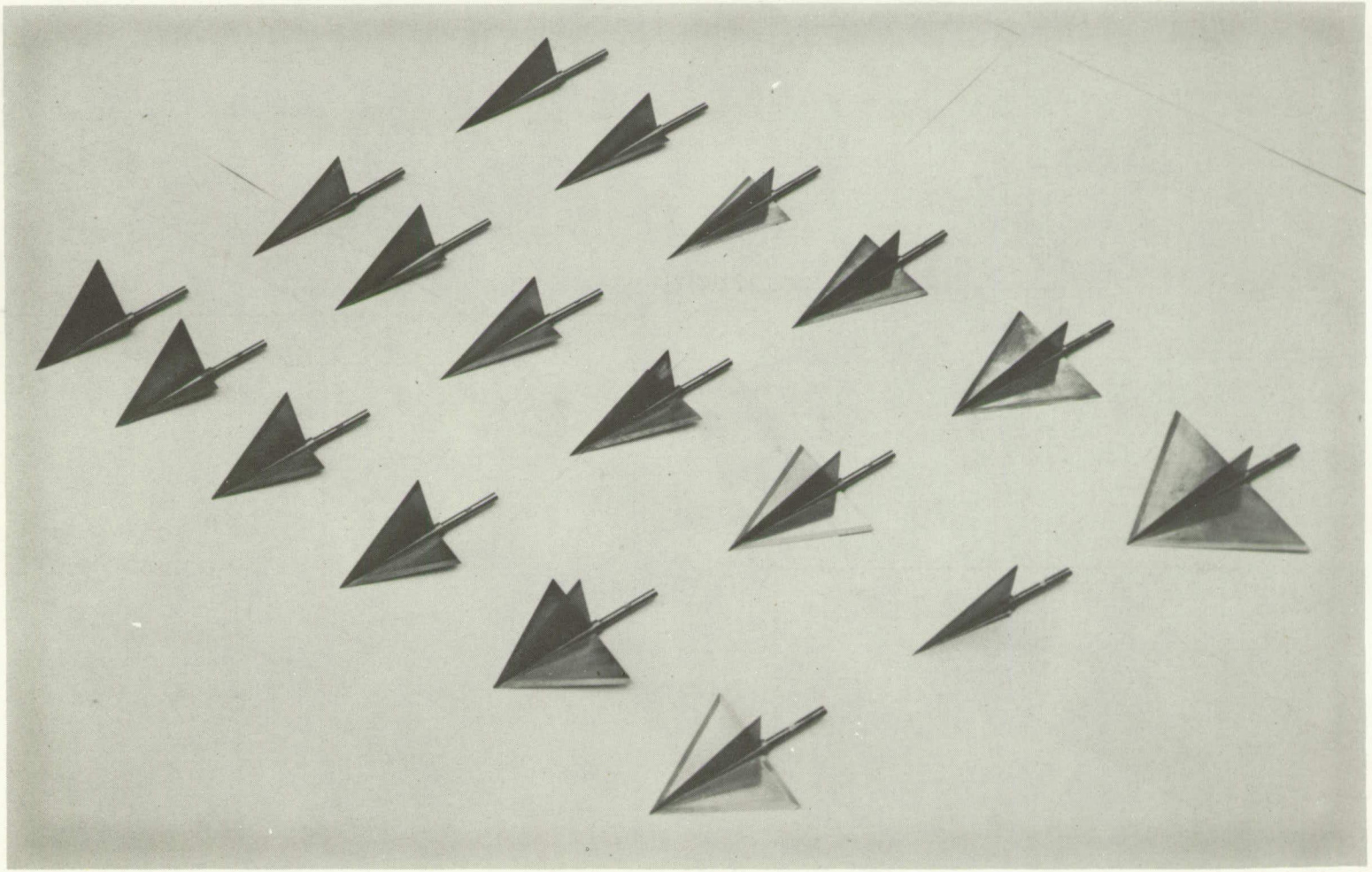

L-84906

Figure 2.- Series of 18 triangular-tail combinations investigated.

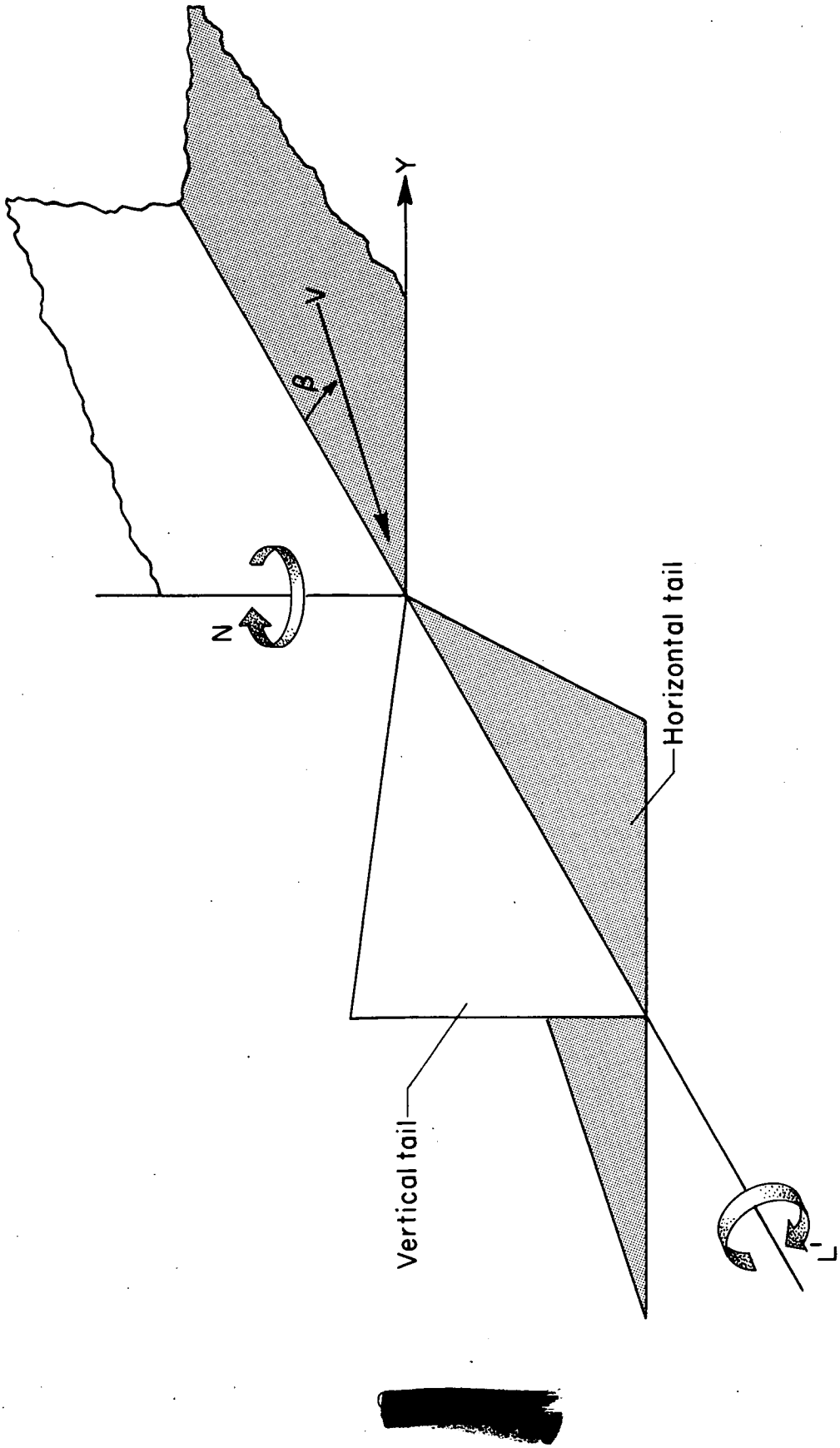

Figure 3.- Sketch of the tail showing positive directions of velocities, forces, and moments.

[redacted]

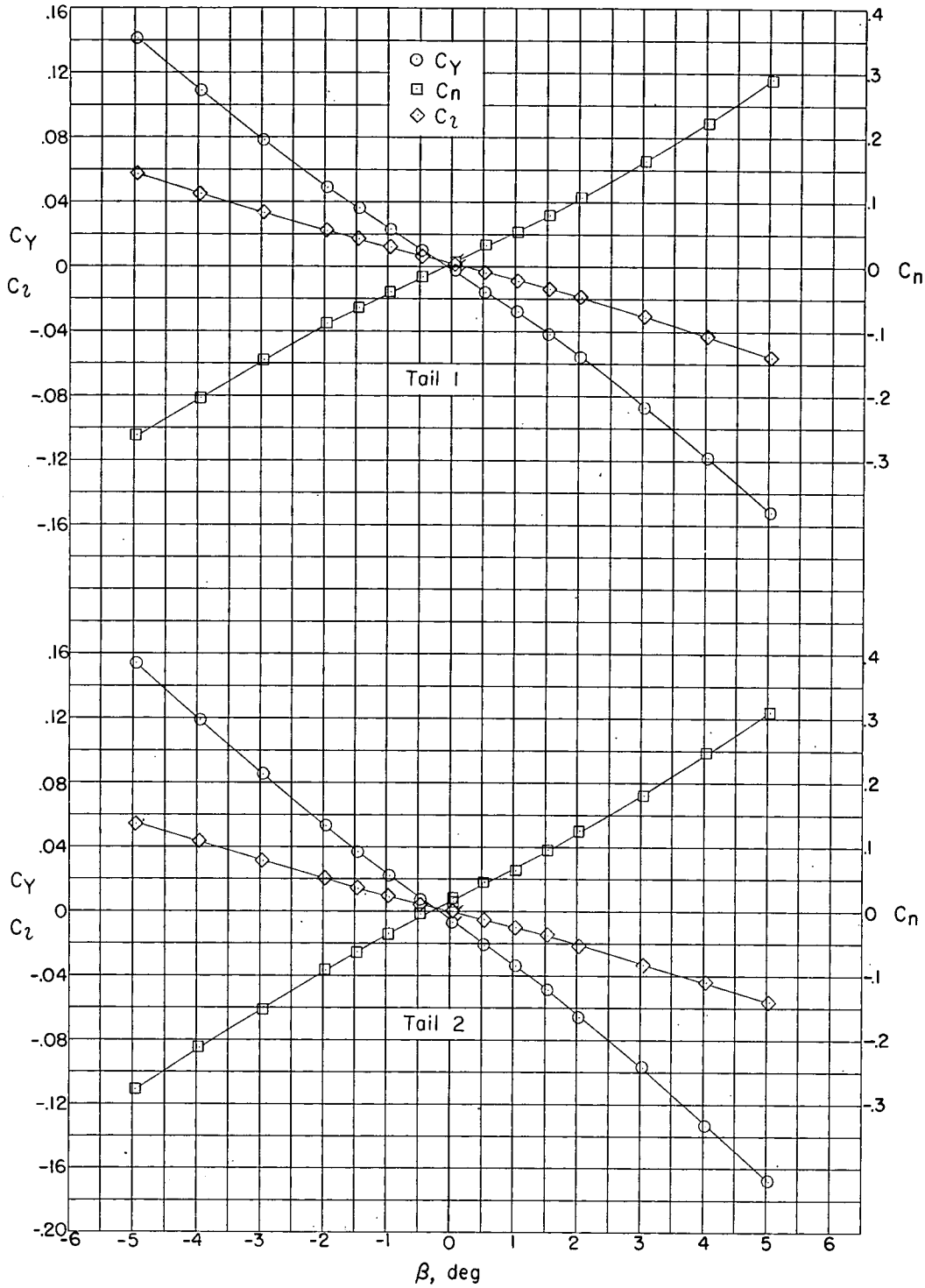

Figure 4.- Lateral-force, yawing-, and rolling-moment coefficients of a triangular vertical- and horizontal-tail combination with subsonic leading edges and supersonic trailing edges as functions of angle of sideslip at M = 1.62. Flagged symbols denote check values.

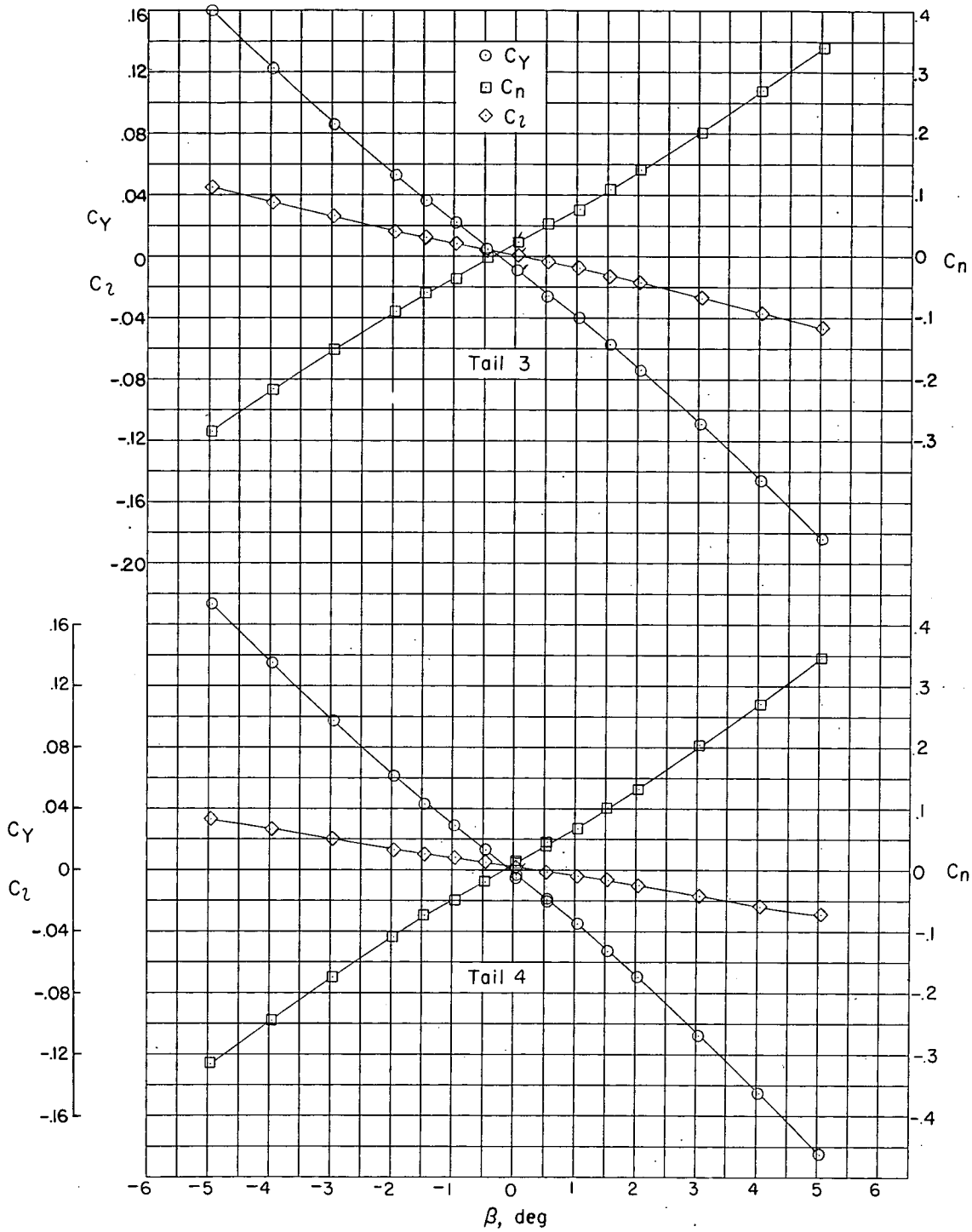

Figure 4.- Continued.

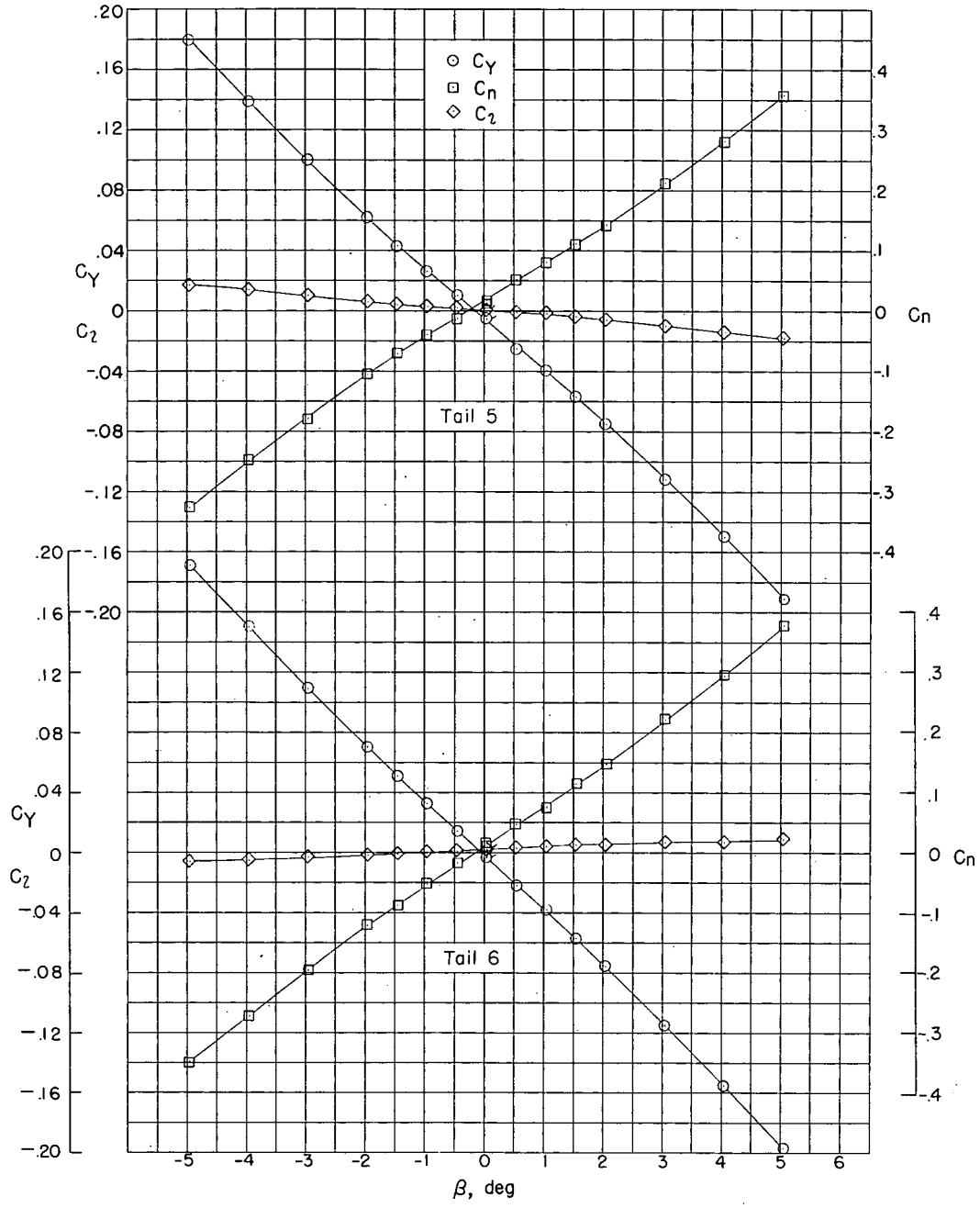

Figure 4.- Continued.

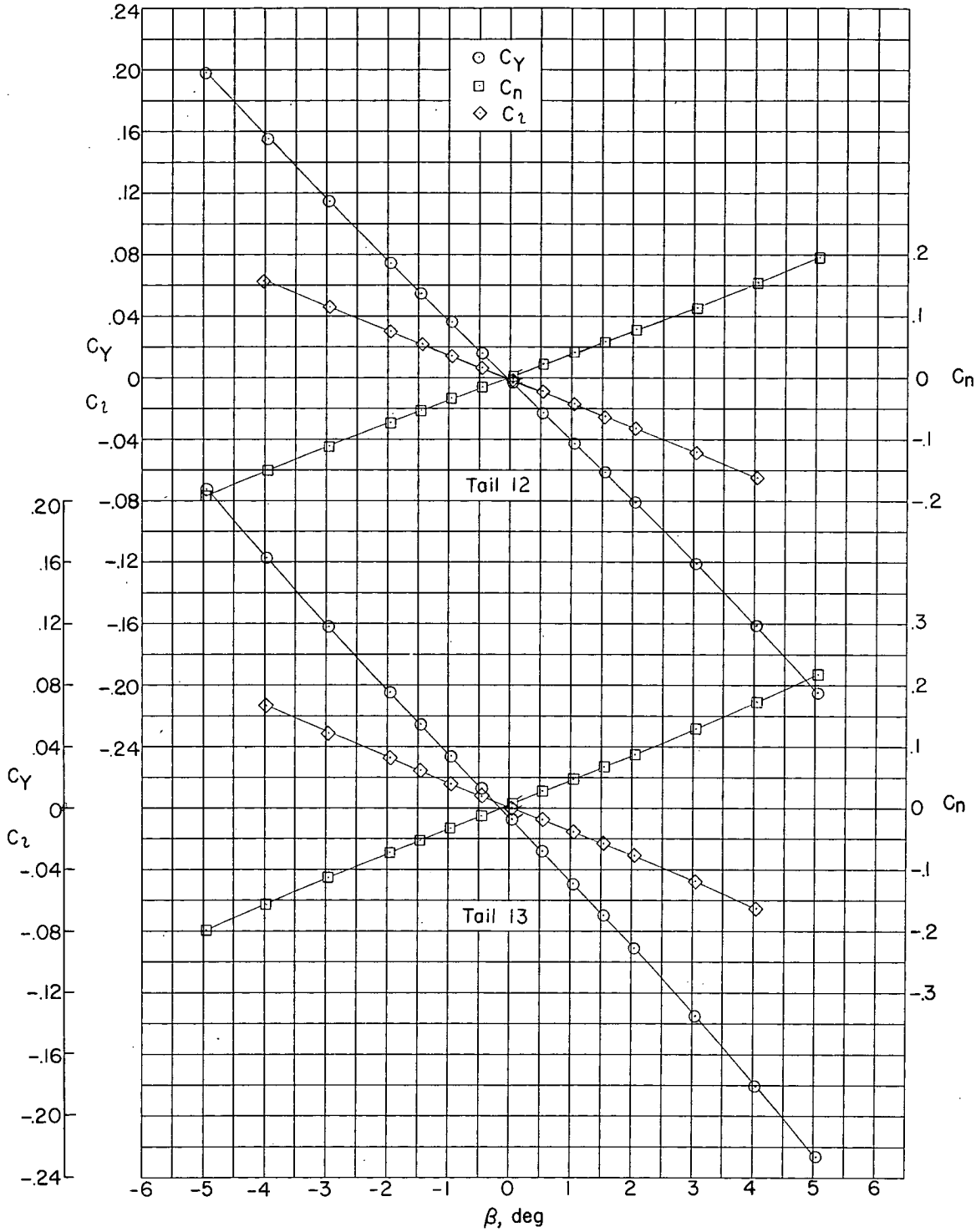

Figure 4.- Continued.

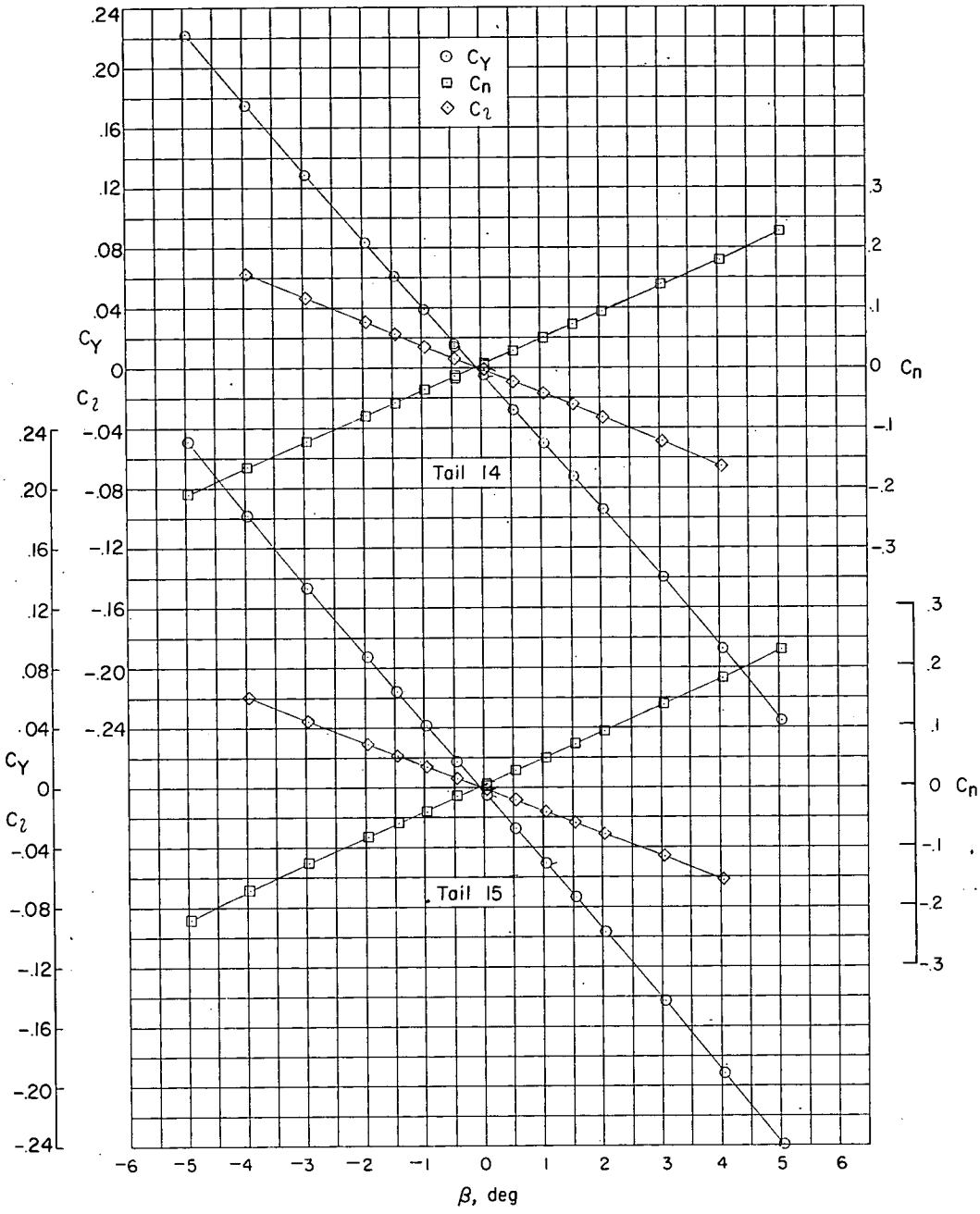

Figure 4.- Continued.

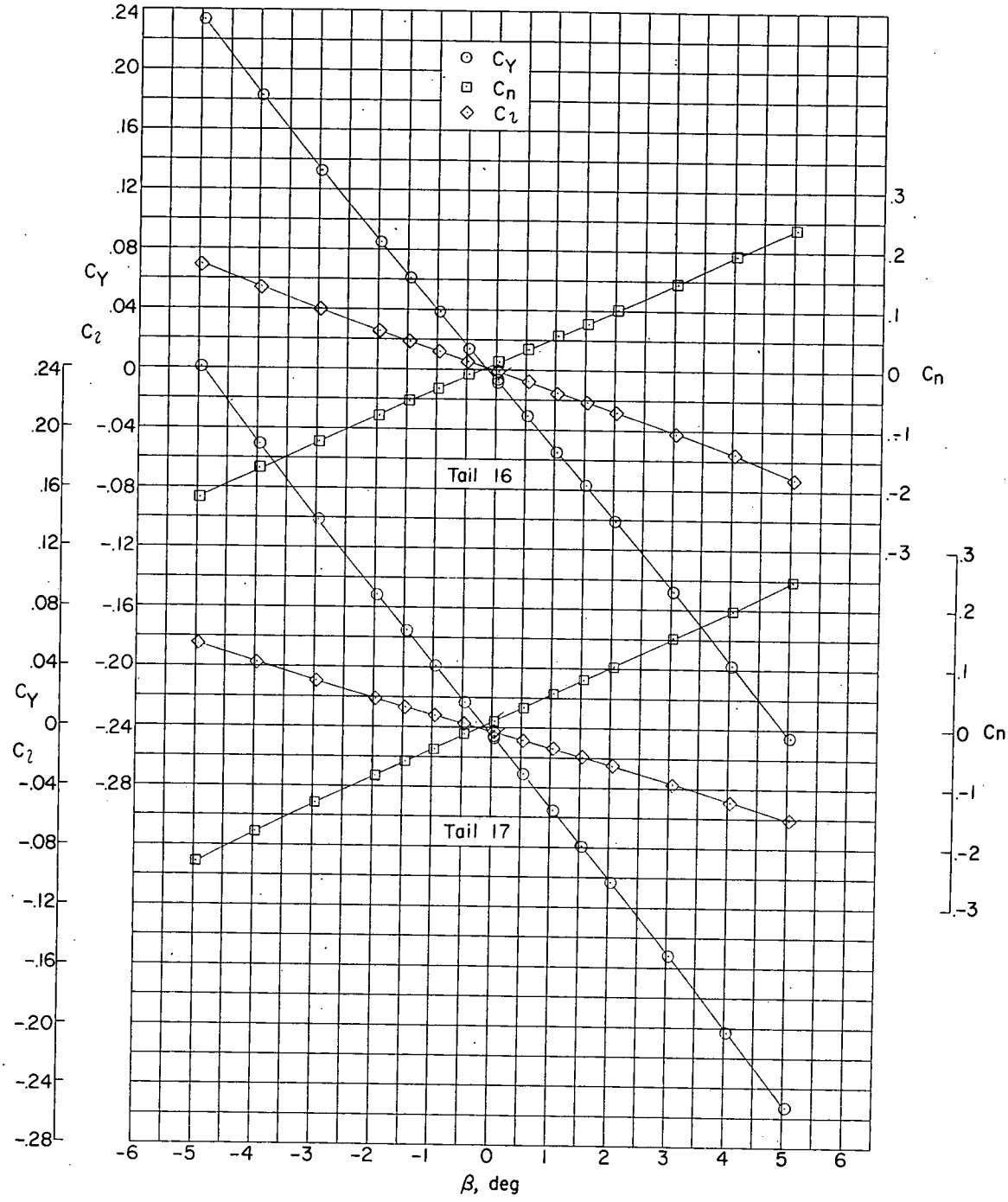

Figure 4.- Concluded.

[redacted]

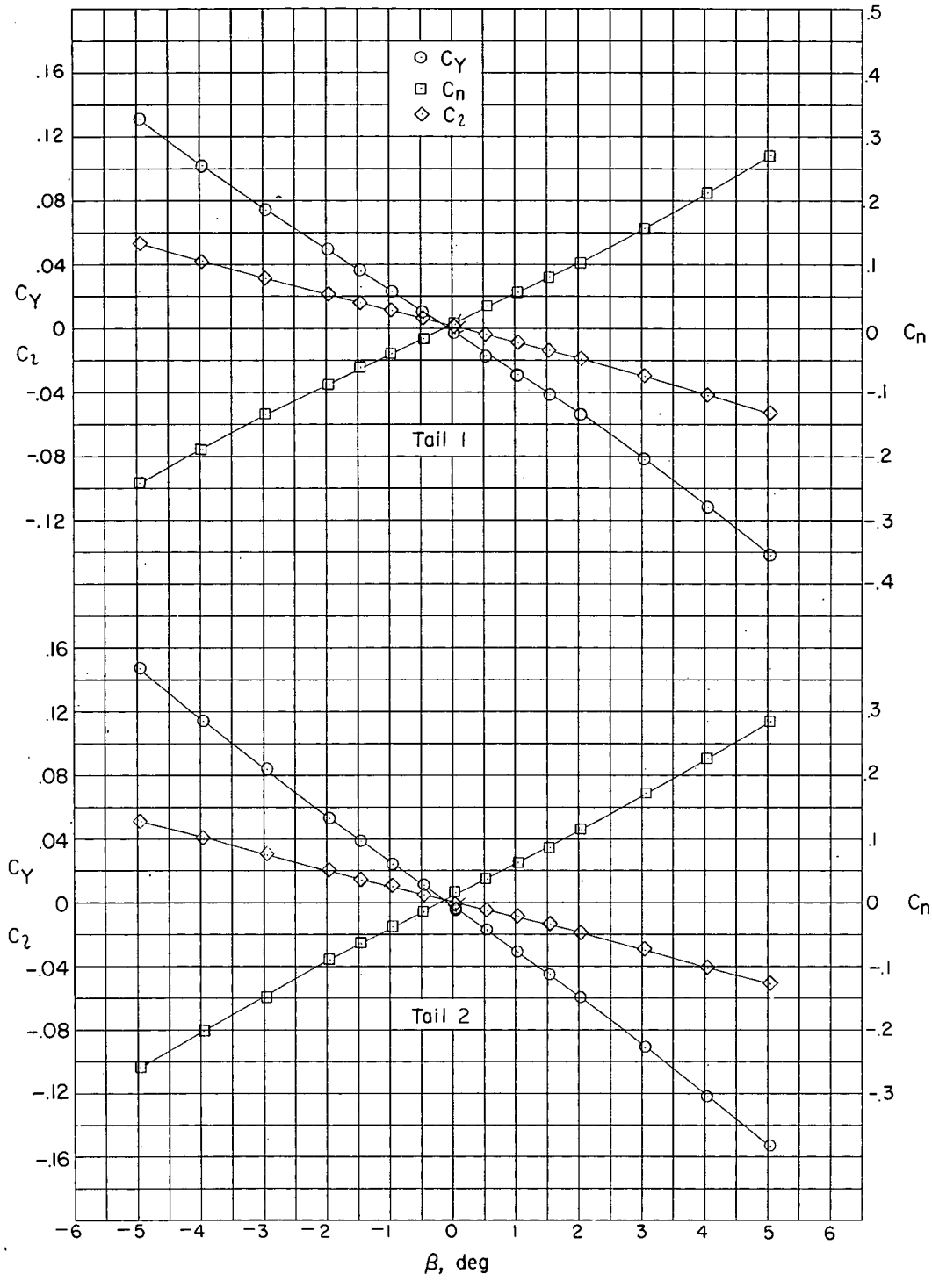

Figure 5.- Lateral-force, yawing-, and rolling-moment coefficients as triangular vertical- and horizontal-tail combination with subsonic leading edges and supersonic trailing edges as functions of angle of sideslip at M = 1.93. Flagged symbols denote check values.

[redacted]

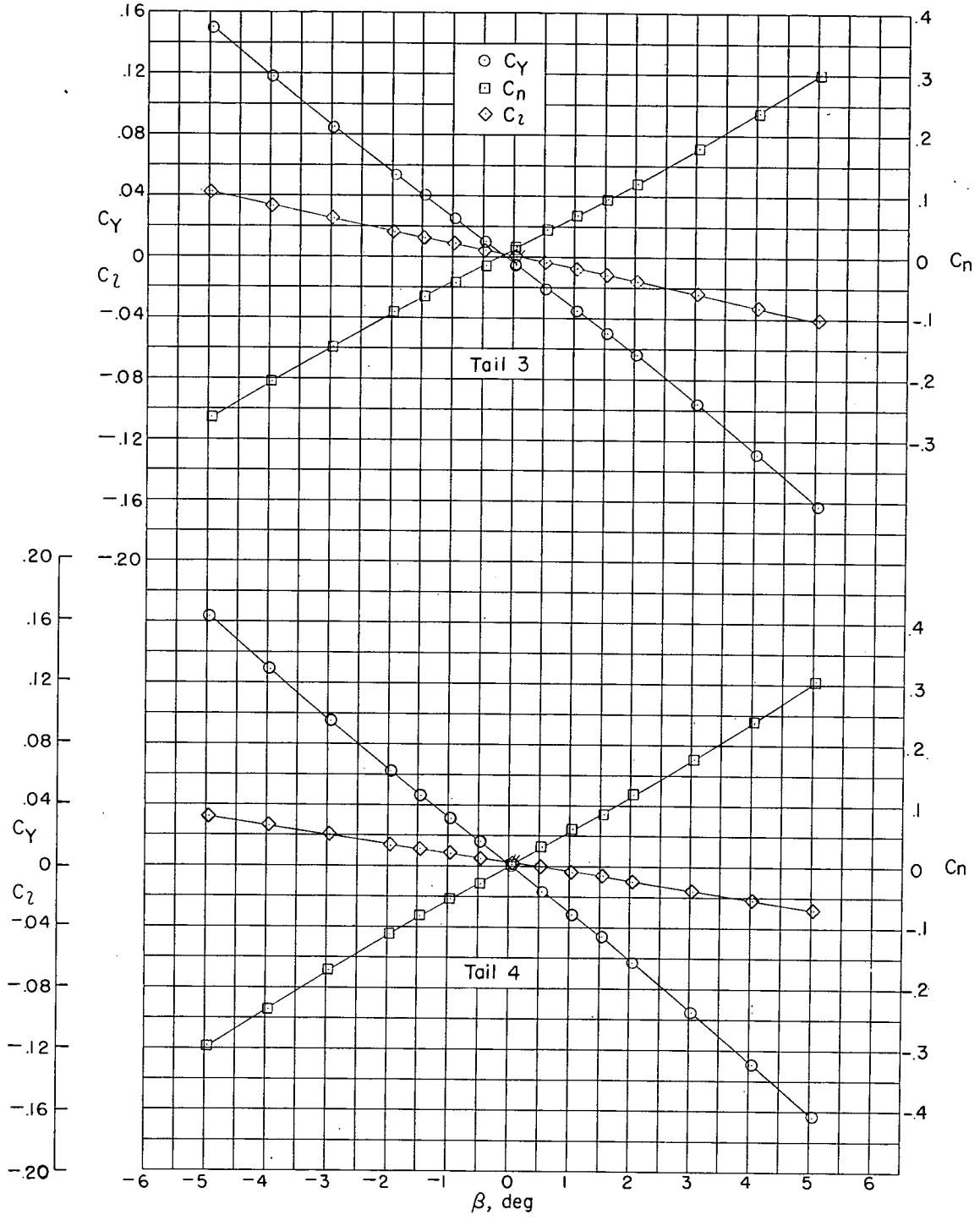

Figure 5.- Continued.

[redacted]

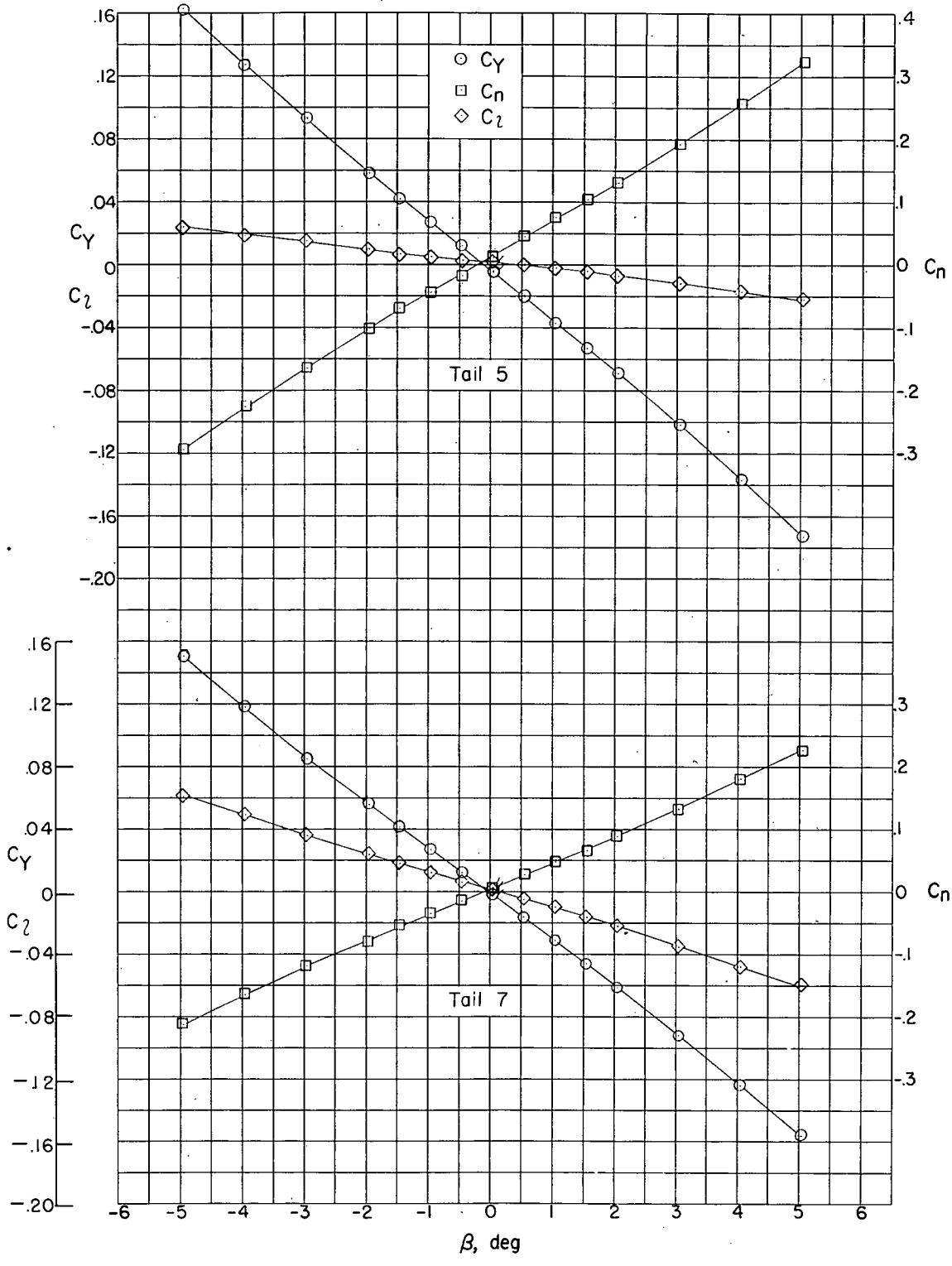

Figure 5.- Continued.

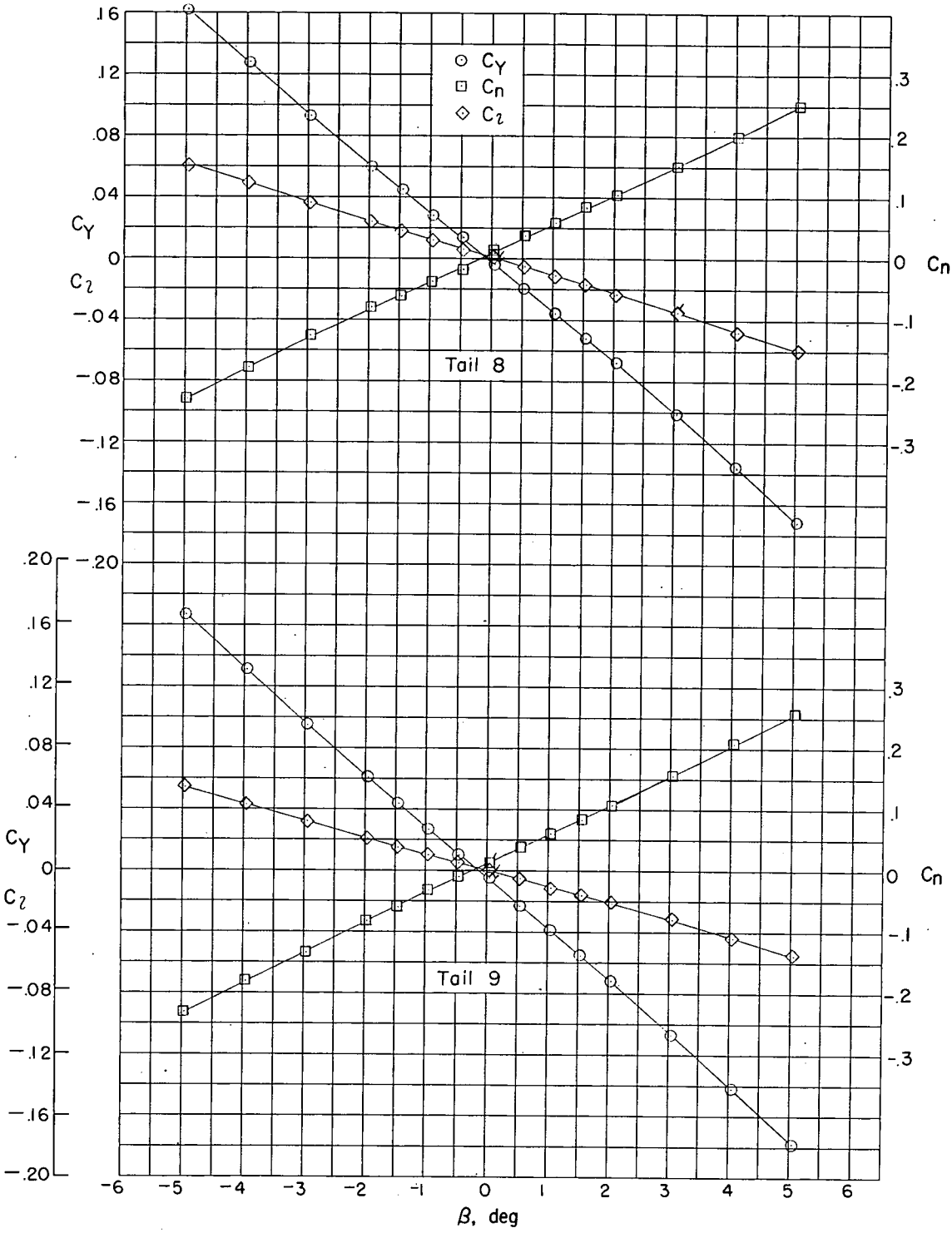

Figure 5.- Continued.

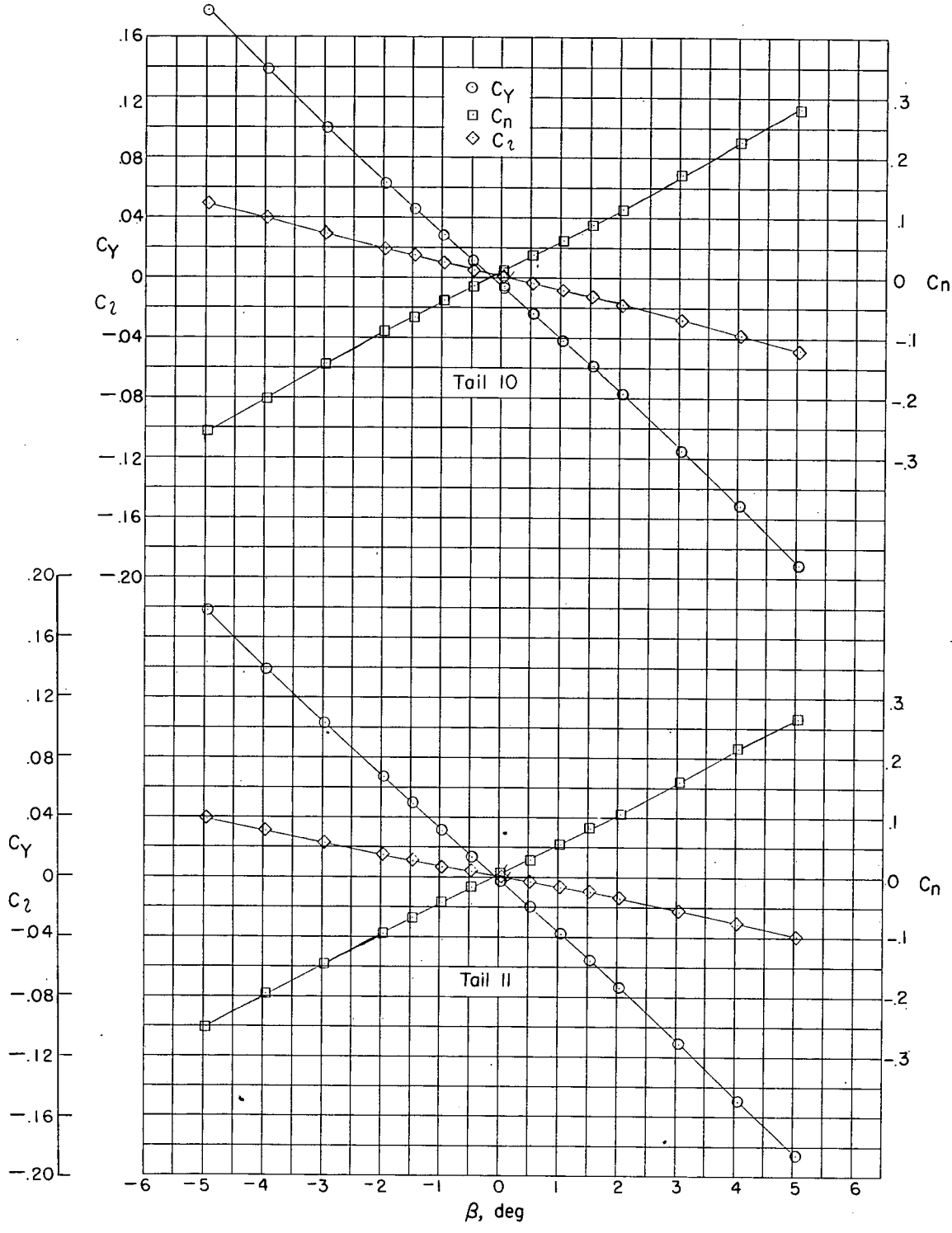

Figure 5.- Concluded.

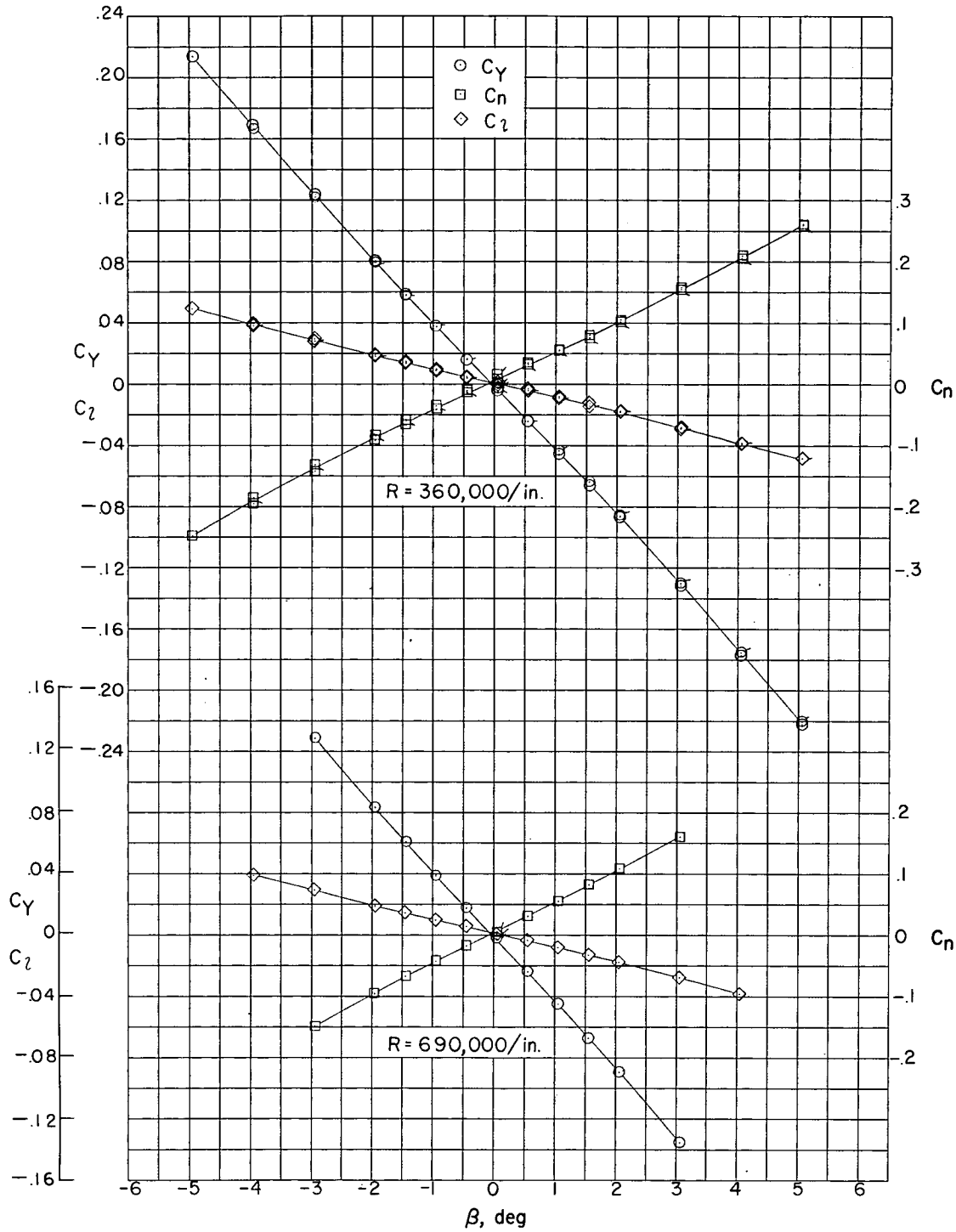

Figure 6.- Lateral-force, yawing-, and rolling-moment coefficients as functions of sideslip angle of tail 18 at M = 1.62 (subsonic leading edge and supersonic trailing edge). R = 360,000 and 690,000 per inch. Flagged symbols denote check values.

[redacted]

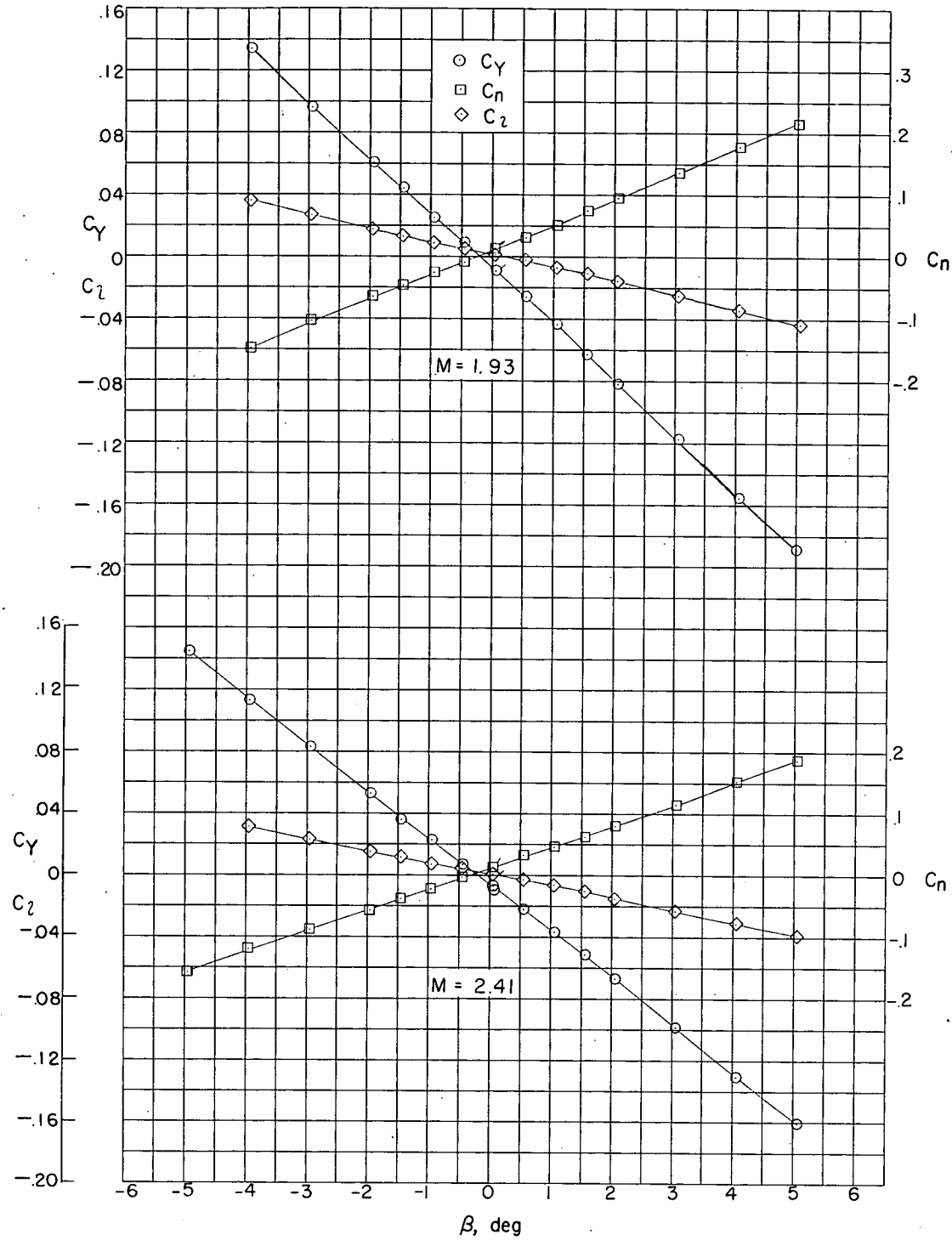

Figure 7.- Lateral-force, yawing-, and rolling-moment coefficients as functions of sideslip angle. Tail 18 at M = 1.93, R = 320,000 per inch (subsonic leading edge and supersonic trailing edge) and at M = 2.41, R = 260,000 per inch (supersonic leading and trailing edges). Flagged symbols denote check values.

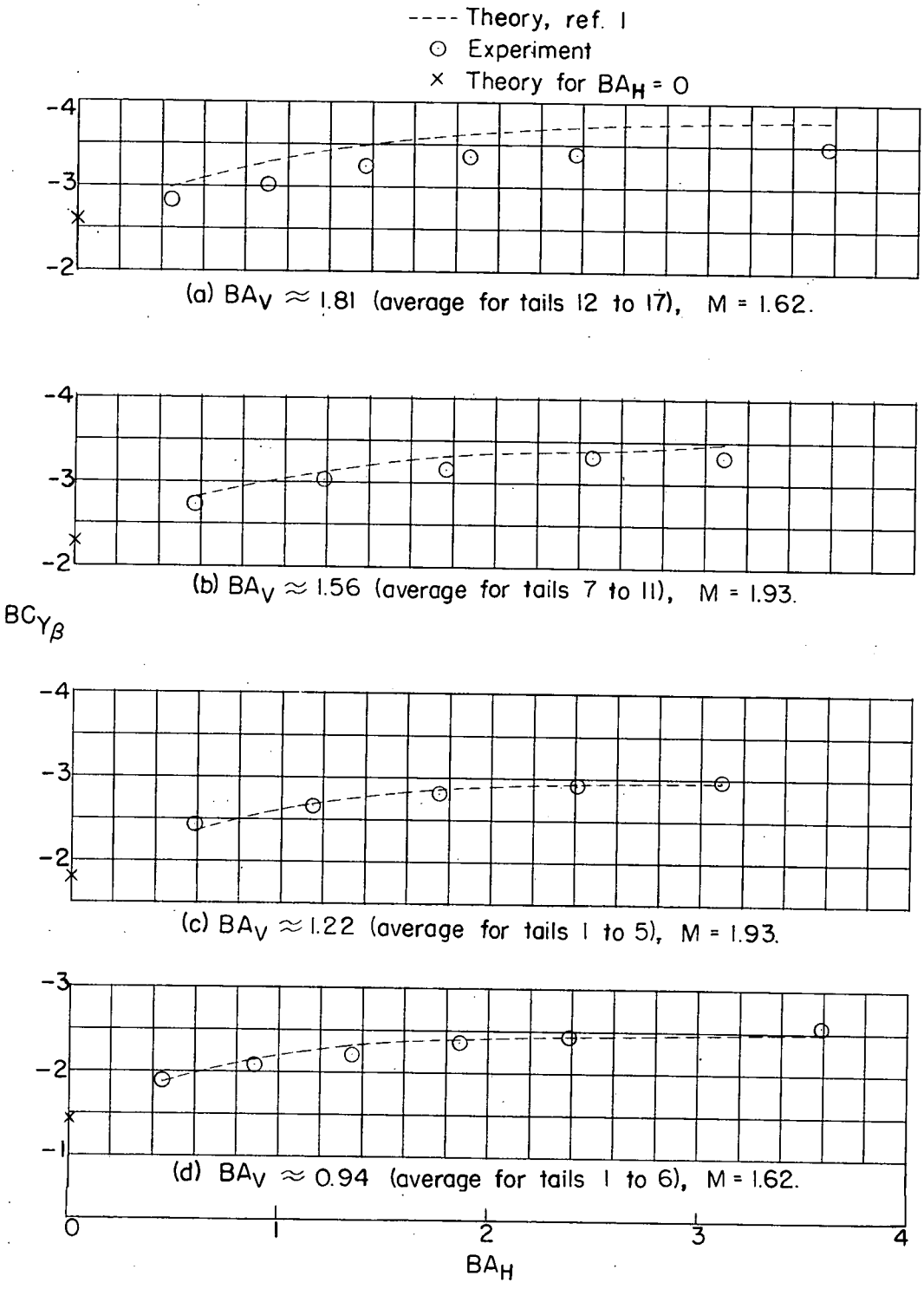

Figure 8.- Comparison between the theoretical and experimental BC_{Y_β} with BA_H for various values of BA_V.

[redacted]

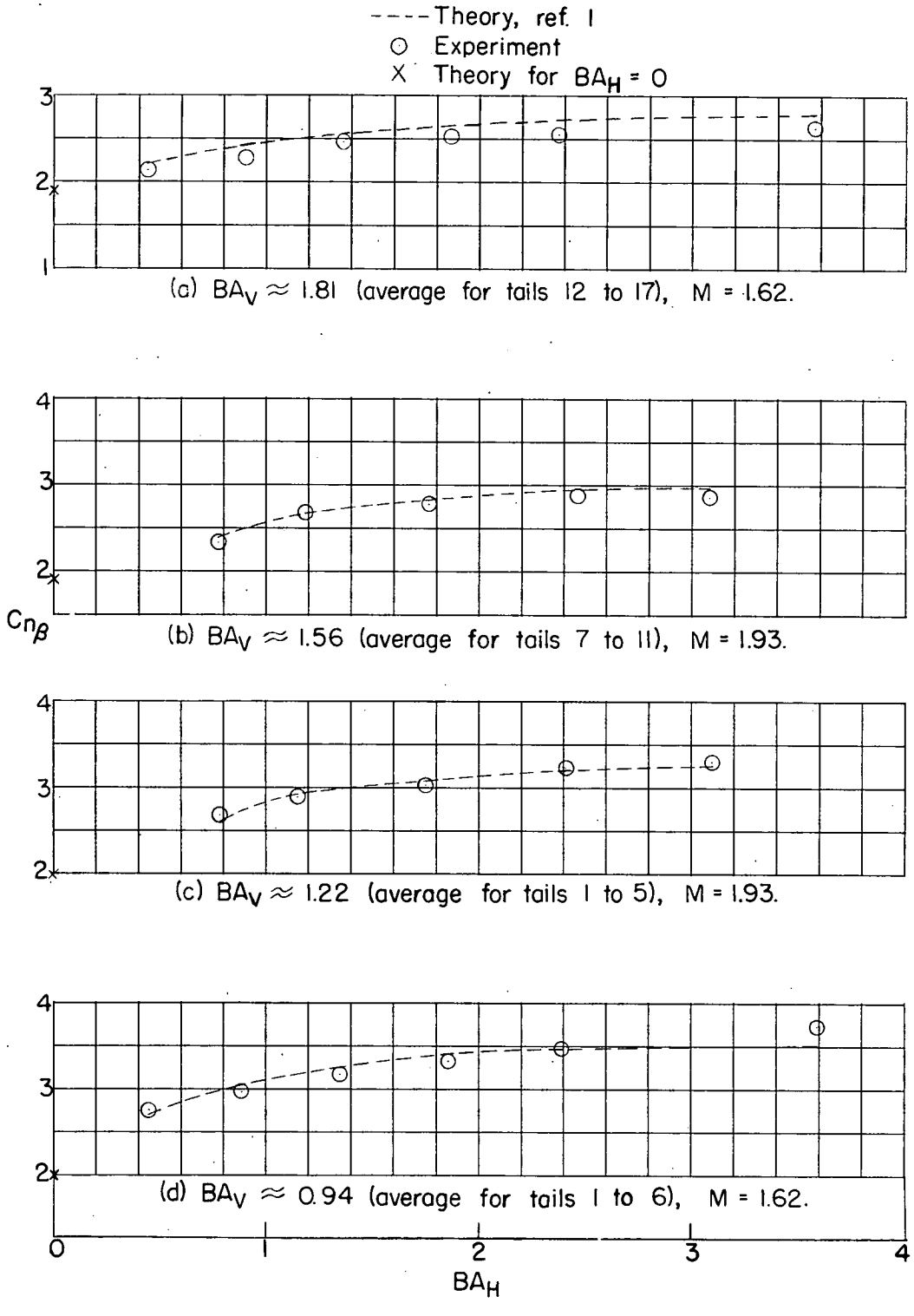

Figure 9.- Comparison between the theoretical and experimental Cn_β with BA_H for various values of BA_V.

[redacted]

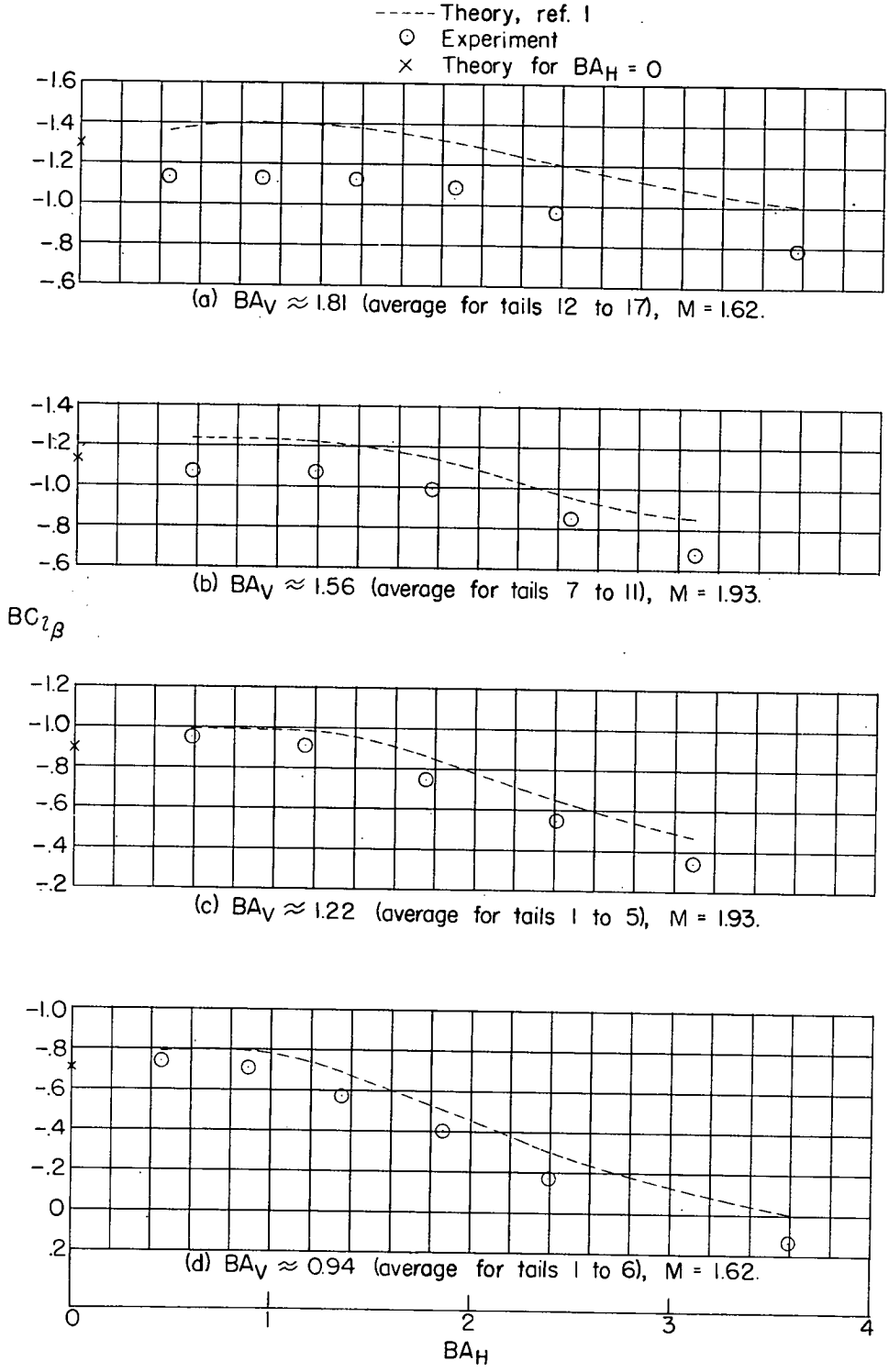

Figure 10.- Comparison between the theoretical and experimental BC_{l_β} with BA_H for various values of BA_V.

[redacted]

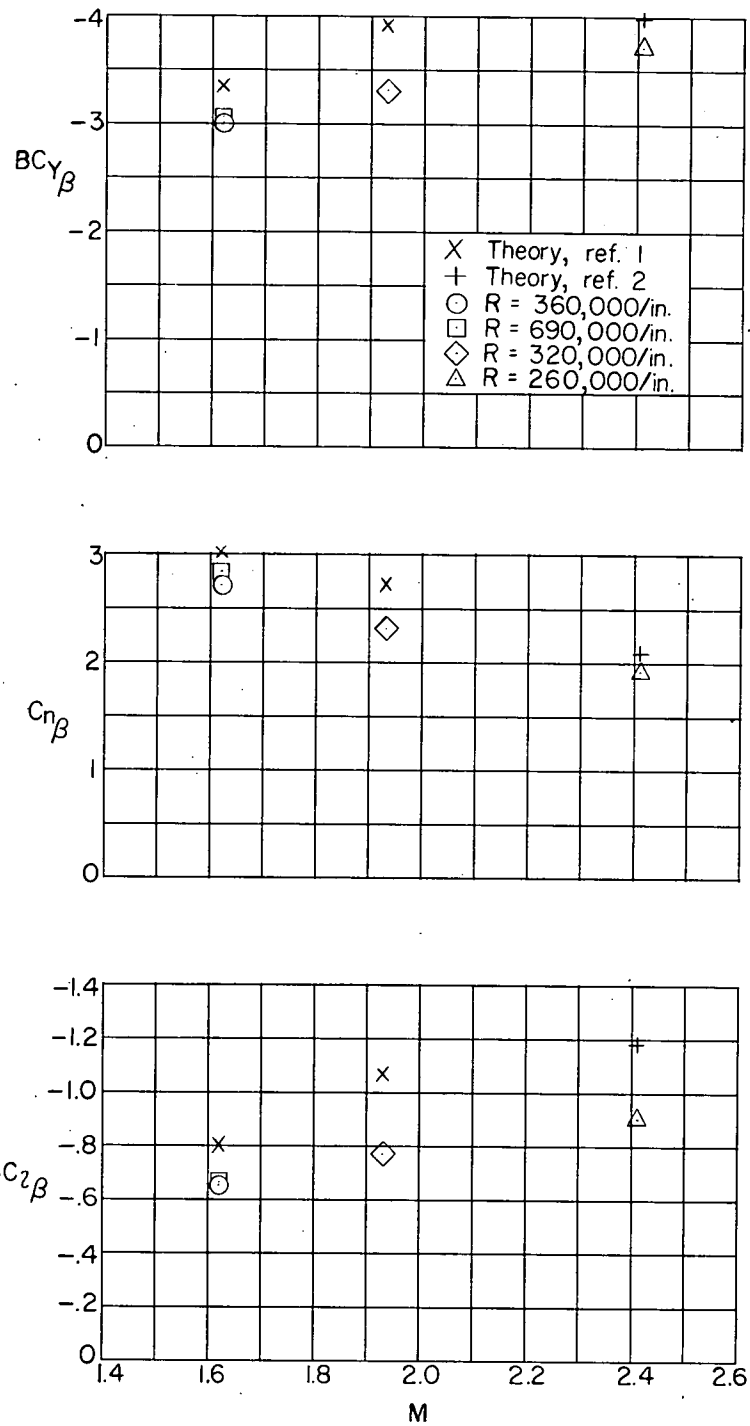

Figure 11.- Comparison between the theoretical and experimental BC_{Y_β}, C_{n_β}, and BC_{l_β} of tail 18 at M = 1.62 and 1.93 (subsonic leading edges and supersonic trailing edges) and M = 2.41 (supersonic leading and trailing edges).